Int. J. Solids Structures Vol. 29, No. 19, pp. 2369–2384, 1992
Printed in Great Britain.

0020-7683/92 $5.00 + .00

POLYGONAL HOLES IN ANISOTROPIC MEDIA

CHYANBIN HWU
Institute of Aeronautics and Astronautics, National Cheng Kung University, Tainan, Taiwan, 70101, Republic of China

(*Received* 2 *September* 1991; *in revised form* 5 *January* 1992)

Abstract—Based upon the solutions obtained by using Stroh's formalism, a general and simplified formula for polygonal holes in anisotropic media is provided in this paper. The polygon used here is a generalized terminology which covers ellipses, polygons and their geometric limits. For some special holes such as ellipses, circles, cracks, triangles, ovals and squares, a further simplified solution is derived. The validity of these formulae is then discussed based on the satisfaction of conformal mapping requirement. The results show that the solutions are exact for (1) anisotropic media containing elliptic holes or cracks, and (2) isotropic media containing general polygonal holes. For general anisotropic media with polygonal holes, the solutions are well approximated if the critical points of the mapping functions are far away from the holes.

1. INTRODUCTION

Because of the anisotropic nature of composite materials, stress concentration due to the presence of holes may be substantially higher in composites than for an equivalent metallic structure. Also, fiber composites generally exhibit near-linear elastic behavior in failure. Therefore, the combination of high stress concentration and the absence of ductile yielding means that composites are relatively intolerant of overloads. Because of this, the study on stress concentration becomes an important topic for composite materials. By classical lamination theory (Jones, 1975) which assumes a rigid bond between adjacent laminae, the composite materials may be modeled as an anisotropic medium. Hence, the study of holes in anisotropic media is critical for the understanding of stress concentration on composites.

Several works such as Savin (1961), Lekhnitskii (1968) and Gao (1991) have been presented in the literature about polygonal holes in isotropic or anisotropic media. However, no exact solutions have been provided for the anisotropic media containing polygonal holes due to the problems of nonconformal mapping. In my recent work (Hwu, 1990), a general and unified solution for anisotropic media with various openings under uniform loading or pure bending has been obtained in an explicit form by using Stroh's formalism (Stroh, 1958). In addition, a real expression has been found for the hoop stress along the hole boundary, which is important for the understanding of anisotropic effect on the stress concentration. Similar to those presented in the literature, the solutions for some openings are not exact due to the fact that the requirement of conformal mapping is not satisfied. Hence, it is interesting to know when the formulae are exact and when they are well approximated. In this paper, we list formulae for polygonal holes in detail, discuss their validity, and verify the discussion by some numerical data. Here, the shape of polygon include ellipses, circles, cracks, triangles, ovals, squares, pentagons, etc. The results show that the solutions are exact for (1) anisotropic media containing elliptic holes or cracks, and (2) isotropic media containing general polygonal holes. For general anisotropic media with polygonal holes, the solutions are well approximated if the critical points of the mapping functions are far away from the holes.

2. POLYGONAL HOLES IN ANISOTROPIC MEDIA

Solutions to the two-dimensional problem of a polygonal hole in an infinite anisotropic medium subjected to uniform loading or pure bending have been obtained by Hwu (1990) through the use of Stroh's formalism. The contour of the hole considered is represented by

$$\left.\begin{aligned} x_1 &= a(\cos\psi + \varepsilon\cos k\psi) \\ x_2 &= a(c\sin\psi - \varepsilon\sin k\psi) \end{aligned}\right\}, \tag{1}$$

where $0 < c \leqslant 1$, and k is an integer. When $\varepsilon = 0$ we obtain an ellipse with semiaxes a and ac. By letting c be equal to zero, an elliptic hole can be made into a crack of length $2a$. In the case that $\varepsilon \neq 0$, a polygon with $k+1$ edges may be obtained by properly choosing the shape parameters a, c, ε and k. Hence, the polygonal holes discussed throughout this paper include ellipse, circle, crack, triangle, oval, square, pentagon, etc.

2.1. *Uniform loading*

The full field solutions of the displacements and stresses for the anisotropic media containing a hole under uniform loading $(\mathbf{t}_1^\infty, \mathbf{t}_2^\infty)$ at infinity are

$$\mathbf{u} = \mathbf{u}^\infty + 2\sum_{l=1,k} \mathrm{Re}\{\mathbf{A}\langle\zeta_\alpha^{-l}\rangle\mathbf{q}_l\}, \quad \boldsymbol{\phi} = \boldsymbol{\phi}^\infty + 2\sum_{l=1,k} \mathrm{Re}\{\mathbf{B}\langle\zeta_\alpha^{-l}\rangle\mathbf{q}_l\}, \tag{2a}$$

where

$$\mathbf{q}_1 = -\tfrac{1}{2}a\mathbf{B}^{-1}(\mathbf{t}_2^\infty - ic\mathbf{t}_1^\infty), \quad \mathbf{q}_k = -\tfrac{1}{2}a\varepsilon\mathbf{B}^{-1}(\mathbf{t}_2^\infty + i\mathbf{t}_1^\infty). \tag{2b}$$

Re denotes the real part of a complex number. The angular brackets $\langle\ \rangle$ stand for the diagonal matrix, i.e.

$$\langle f_\alpha\rangle = \mathrm{diag}\,[f_1, f_2, f_3]$$

in which each component is varied according to the Greek index α. $\mathbf{u}$ and $\boldsymbol{\phi}$ represent the displacement and stress function, respectively. The superscript ∞ denotes the value at infinity. $\mathbf{A}$ and $\mathbf{B}$ are 3×3 complex matrices composed of elasticity constants. ζ_α is related to z_α $(= x_1 + p_\alpha x_2)$ by the following transformation function:

$$z_\alpha = \frac{a}{2}\left\{(1 - ip_\alpha c)\zeta_\alpha + (1 + ip_\alpha c)\frac{1}{\zeta_\alpha} + \varepsilon(1 + ip_\alpha)\zeta_\alpha^k + \varepsilon(1 - ip_\alpha)\frac{1}{\zeta_\alpha^k}\right\}, \tag{3}$$

where p_α is the material eigenvalue.

As for the hoop stress σ_{nn} along the hole boundary, a real form solution has been obtained as follows:

$$\sigma_{nn} = \mathbf{n}^{\mathrm{T}}(\theta)\mathbf{t}_n, \quad \mathbf{t}_n = \cos\theta\mathbf{t}_1^\infty + \sin\theta\mathbf{t}_2^\infty$$

$$+ \frac{1}{\rho}\mathbf{N}_3(\theta)\mathbf{L}^{-1}\{[\rho\cos\theta - (1+c)a\sin\psi]\mathbf{t}_1^\infty + [\rho\sin\theta + (1+c)a\cos\psi]\mathbf{t}_2^\infty\}$$

$$+ [\mathbf{N}_1^{\mathrm{T}}(\theta) - \mathbf{N}_3(\theta)\mathbf{S}\mathbf{L}^{-1}]\{-\sin\theta\mathbf{t}_1^\infty + \cos\theta\mathbf{t}_2^\infty\}, \tag{4}$$

where $\mathbf{N}_i(\theta)$, $i = 1, 2, 3$ and $\mathbf{S}$, $\mathbf{L}$ are 3×3 real matrices composed of elasticity constants. $\mathbf{n}(\theta)$ is the unit vector tangent to the hole boundary. θ is the angle directed counterclockwise from the positive x_1-axis to the direction of $\mathbf{n}(\theta)$, which is related to ψ by

$$\rho\cos\theta = a(\sin\psi + k\varepsilon\sin k\psi), \quad \rho\sin\theta = -a(c\cos\psi - k\varepsilon\cos k\psi), \tag{5a}$$

where

$$\rho^2 = a^2\{k^2\varepsilon^2 + \sin^2\psi + c^2\cos^2\psi + 2k\varepsilon\sin\psi\sin k\psi - 2ck\varepsilon\cos\psi\cos k\psi\}. \tag{5b}$$

2.2. *Pure bending*

The full field solutions of the displacements and stresses for the hole subjected to pure bending M in a direction at an angle α with the positive x_1-axis, are

$$\mathbf{u} = \mathbf{u}^{\infty} + 2\sum_{\substack{l=0,2k-1\\k+1,2k}} \mathrm{Re}\{\mathbf{A}\langle\zeta_\alpha^{-l}\rangle\mathbf{q}_l\}, \quad \boldsymbol{\phi} = \boldsymbol{\phi}^{\infty} + 2\sum_{\substack{l=0,2k-1\\k+1,2k}} \mathrm{Re}\{\mathbf{B}\langle\zeta_\alpha^{-l}\rangle\mathbf{q}_l\}, \tag{6a}$$

where

$$\mathbf{q}_l = \frac{Ma^2}{4I}(c_l + \mathrm{i}s_l)\mathbf{B}^{-1}\mathbf{n}(\alpha), \tag{6b}$$

and

$$\begin{aligned}
c_2 &= \frac{1}{4}[1 - c^2 - (1+c^2)\cos 2\alpha], & s_2 &= \frac{-c}{2}\sin 2\alpha,\\
c_{k-1} &= \frac{\varepsilon}{2}[(1-c) - (1+c)\cos 2\alpha], & s_{k-1} &= \frac{\varepsilon}{2}(1+c)\sin 2\alpha,\\
c_{k+1} &= \frac{\varepsilon}{2}[1 + c) - (1-c)\cos 2\alpha], & s_{k+1} &= \frac{\varepsilon}{2}(1-c)\sin 2\alpha,\\
c_{2k} &= -\frac{\varepsilon^2}{2}\cos 2\alpha, & s_{2k} &= \frac{\varepsilon^2}{2}\sin 2\alpha.
\end{aligned} \tag{6c}$$

I is the moment inertia of the plate cross section normal to the loaded axis. A real form solution for the hoop stress σ_{nn} along the hole boundary has been obtained as

$$\sigma_{nn}\Big/\left(\frac{Ma}{I}\right) = s_0^*\cos^2(\theta-\alpha) + \frac{ac^*}{2\rho}\mathbf{n}^{\mathrm{T}}(\theta)\mathbf{N}_3(\theta)\mathbf{L}^{-1}\mathbf{n}(\alpha) + \frac{as^*}{2\rho}\mathbf{n}^{\mathrm{T}}(\theta)[\mathbf{N}_1^{\mathrm{T}}(\theta) - \mathbf{N}_3(\theta)\mathbf{S}\mathbf{L}^{-1}]\mathbf{n}(\alpha), \tag{7a}$$

where

$$\begin{aligned}
s_0^* &= \sin(\psi-\alpha) - \varepsilon\sin(k\psi+\alpha) - (1-c)\cos\alpha\sin\psi,\\
s^* &= -\sum_{\substack{l=2k\\k+1,2k-1}} l(c_l\sin l\psi + s_l\cos l\psi),\\
c^* &= -\sum_{\substack{l=2k\\k+1,2k-1}} l(s_l\sin l\psi + c_l\cos l\psi).
\end{aligned} \tag{7b}$$

Note that the solutions presented in (2) and (6) are much simpler than those shown in Hwu (1990) since the following identities

$$\mathbf{A}^{\mathrm{T}} + \mathbf{B}^{\mathrm{T}}\mathbf{L}^{-1}\mathbf{S}^{\mathrm{T}} = \tfrac{1}{2}\mathbf{B}^{-1}, \quad 2\mathbf{B}^{\mathrm{T}}\mathbf{L}^{-1} = \mathrm{i}\mathbf{B}^{-1},$$

which can easily be derived by the definitions of S and L, have been used to simplify the formula.

3. FORMULAE FOR HOMOGENEOUS MEDIA

For a plate without any holes subjected to an external loading applied at infinity, the displacement $\mathbf{u}^\infty$ and stress function $\boldsymbol{\phi}^\infty$, which are necessary for the completeness of the formulae, can be determined by the following procedures:

(1) The stress field σ_{ij}^∞ is obtained under the requirements that the infinity loading conditions and the equilibrium equations should be satisfied. Moreover, for two-dimensional problems, σ_{ij}^∞ have to be prescribed in such a way that $\varepsilon_{33}^\infty = 0$.

(2) By $\sigma_{i1} = -\phi_{i,2}$ and $\sigma_{i2} = \phi_{i,1}$, integrations of the stresses with respect to x_1 and x_2 will lead to the stress function $\boldsymbol{\phi}^\infty$.

(3) The associated strain field ε_{ij}^∞ is then obtained by using the reduced constitutive law which implies that $\varepsilon_{33}^\infty = 0$ and is expressed as

$$\varepsilon_i = \sum_{j \neq 3} \hat{S}_{ij}\sigma_j, \quad i \neq 3, \tag{8a}$$

where $\hat{S}_{ij}$ is the reduced elastic compliance and is related to the compliance S_{ij} by

$$\hat{S}_{ij} = S_{ij} - S_{i3}S_{3j}/S_{33}. \tag{8b}$$

ε_i and σ_i ranging from 1 to 6 are the contracted notations of ε_{ij} and σ_{ij}. The correctness of ε_{ij}^∞ and σ_{ij}^∞ should be checked by the following compatibility equations:

$$\left.\begin{aligned} \frac{\partial \varepsilon_{23}}{\partial x_1} &= \frac{\partial \varepsilon_{31}}{\partial x_2} \\ 2\frac{\partial^2 \varepsilon_{12}}{\partial x_1 \partial x_2} &= \frac{\partial^2 \varepsilon_{11}}{\partial x_2^2} + \frac{\partial^2 \varepsilon_{22}}{\partial x_1^2} \end{aligned}\right\}. \tag{9}$$

If the compatibility equations are not satisfied, one should return to step (1) and look for another possible equilibrated stress σ_{ij}^∞. If no solutions can satisfy all the above requirements, the assumption of two-dimensional deformation should be modified, which will not be considered in this paper.

(4) The displacement $\mathbf{u}^\infty$ is then obtained by integration of the following reduced strain–displacement equations for two-dimensional problems,

$$\varepsilon_{11} = \frac{\partial u_1}{\partial x_1}, \quad \varepsilon_{22} = \frac{\partial u_2}{\partial x_2}, \quad 2\varepsilon_{12} = \frac{\partial u_1}{\partial x_2} + \frac{\partial u_2}{\partial x_1}, \quad 2\varepsilon_{23} = \frac{\partial u_3}{\partial x_2}, \quad 2\varepsilon_{13} = \frac{\partial u_3}{\partial x_1}.$$

That is,

$$u_1 = \int \varepsilon_{11}\, \mathrm{d}x_1, \quad u_2 = \int \varepsilon_{22}\, \mathrm{d}x_2, \quad u_3 = \int 2\varepsilon_{23}\, \mathrm{d}x_2 \tag{10a}$$

in which the integration constants can be determined by

$$2\varepsilon_{12} = \frac{\partial u_1}{\partial x_2} + \frac{\partial u_2}{\partial x_1}, \quad 2\varepsilon_{13} = \frac{\partial u_3}{\partial x_1}, \tag{10b}$$

and the neglect of rigid body translation and rotation.

By the procedures described above, we now list the solutions of $\mathbf{u}^\infty$, $\boldsymbol{\phi}^\infty$ for the two-dimensional anisotropic plate without holes subjected to uniform loading or pure bending at infinity.

3.1. *Uniform loading*

$$\mathbf{u}^{\infty} = x_1\boldsymbol{\varepsilon}_1^{\infty} + x_2\boldsymbol{\varepsilon}_2^{\infty}, \quad \boldsymbol{\phi}^{\infty} = x_1\mathbf{t}_2^{\infty} - x_2\mathbf{t}_1^{\infty}, \tag{11a}$$

where

$$\mathbf{t}_1^{\infty} = \begin{Bmatrix} \sigma_{11}^{\infty} \\ \sigma_{12}^{\infty} \\ \sigma_{13}^{\infty} \end{Bmatrix}, \quad \mathbf{t}_2^{\infty} = \begin{Bmatrix} \sigma_{21}^{\infty} \\ \sigma_{22}^{\infty} \\ \sigma_{23}^{\infty} \end{Bmatrix}, \quad \boldsymbol{\varepsilon}_1^{\infty} = \begin{Bmatrix} \varepsilon_1^{\infty} \\ \varepsilon_{12}^{\infty} \\ 2\varepsilon_{13}^{\infty} \end{Bmatrix}, \quad \boldsymbol{\varepsilon}_2^{\infty} = \begin{Bmatrix} \varepsilon_{21}^{\infty} \\ \varepsilon_{22}^{\infty} \\ 2\varepsilon_{23}^{\infty} \end{Bmatrix}. \tag{11b}$$

In the above, σ_{ij}^{∞} are given and $\varepsilon_{ij}^{\infty}$ can be determined by using the reduced stress–strain relation (8). The simplified solutions for some special loading conditions are listed in the following.

3.1.1. *Unidirectional tension.* ($\sigma_{11}^{\infty} = \sigma^{\infty}\cos^2\alpha$, $\sigma_{22}^{\infty} = \sigma^{\infty}\sin^2\alpha$, $\sigma_{12}^{\infty} = \sigma^{\infty}\cos\alpha\sin\alpha$)

$$\begin{aligned} \mathbf{t}_1^{\infty} &= \sigma^{\infty}\cos\alpha\mathbf{n}(\alpha), \quad \mathbf{t}_2^{\infty} = \sigma^{\infty}\sin\alpha\mathbf{n}(\alpha), \\ \boldsymbol{\varepsilon}_1^{\infty} &= \sigma^{\infty}\{\cos^2\alpha\mathbf{S}_1 + \sin^2\alpha\mathbf{S}_2 + \cos\alpha\sin\alpha\mathbf{S}_6\}, \\ \boldsymbol{\varepsilon}_2^{\infty} &= \sigma^{\infty}\{\cos^2\alpha\mathbf{S}_1^* + \sin^2\alpha\mathbf{S}_2^* + \cos\alpha\sin\alpha\mathbf{S}_6^*\}, \end{aligned} \tag{12a}$$

where

$$\mathbf{S}_i = \begin{Bmatrix} \hat{S}_{1i} \\ \frac{1}{2}\hat{S}_{6i} \\ \hat{S}_{5i} \end{Bmatrix}, \quad \mathbf{S}_i^* = \begin{Bmatrix} \frac{1}{2}\hat{S}_{6i} \\ \hat{S}_{2i} \\ \hat{S}_{4i} \end{Bmatrix}, \quad i = 1, 2, 6. \tag{12b}$$

3.1.2. *Biaxial loading.* ($\sigma_{11}^{\infty} = \sigma_1^{\infty}$, $\sigma_{22}^{\infty} = \sigma_2^{\infty}$)

$$\mathbf{t}_1^{\infty} = \sigma_1^{\infty}\mathbf{i}_1, \quad \mathbf{t}_2^{\infty} = \sigma_2^{\infty}\mathbf{i}_2, \quad \boldsymbol{\varepsilon}_1^{\infty} = \sigma_1^{\infty}\mathbf{S}_1 + \sigma_2^{\infty}\mathbf{S}_2, \quad \boldsymbol{\varepsilon}_2^{\infty} = \sigma_1^{\infty}\mathbf{S}_1^* + \sigma_2^{\infty}\mathbf{S}_2^*, \tag{13a}$$

where

$$\mathbf{i}_1 = \begin{Bmatrix} 1 \\ 0 \\ 0 \end{Bmatrix}, \quad \mathbf{i}_2 = \begin{Bmatrix} 0 \\ 1 \\ 0 \end{Bmatrix}. \tag{13b}$$

3.1.3. *Pure shear.* ($\sigma_{12}^{\infty} = \tau^{\infty}$)

$$\mathbf{t}_1^{\infty} = \tau^{\infty}\mathbf{i}_2, \quad \mathbf{t}_2^{\infty} = \tau^{\infty}\mathbf{i}_1, \quad \boldsymbol{\varepsilon}_1^{\infty} = \tau^{\infty}\mathbf{S}_6, \quad \boldsymbol{\varepsilon}_2^{\infty} = \tau^{\infty}\mathbf{S}_6^*. \tag{14}$$

3.1.4. *Anti-plane shear.* ($\sigma_{13}^{\infty} = \tau^{\infty}$ or $\sigma_{23}^{\infty} = \tau^{\infty}$)

$$\mathbf{t}_1^{\infty} = \tau^{\infty}\mathbf{i}_3, \quad \mathbf{t}_2^{\infty} = \mathbf{0}, \quad \boldsymbol{\varepsilon}_1^{\infty} = \tau^{\infty}\mathbf{S}_5, \quad \boldsymbol{\varepsilon}_2^{\infty} = \tau^{\infty}\mathbf{S}_5^*, \tag{15a}$$

or

$$\mathbf{t}_1^{\infty} = \mathbf{0}, \quad \mathbf{t}_2^{\infty} = \tau^{\infty}\mathbf{i}_3, \quad \boldsymbol{\varepsilon}_1^{\infty} = \tau^{\infty}\mathbf{S}_4, \quad \boldsymbol{\varepsilon}_2^{\infty} = \tau^{\infty}\mathbf{S}_4^*, \tag{15b}$$

where

$$\mathbf{i}_3 = \begin{Bmatrix} 0 \\ 0 \\ 1 \end{Bmatrix}. \tag{15c}$$

3.2. *Pure bending*

$$\left.\begin{aligned} \mathbf{u}^{\infty} &= \frac{-M}{2I}(\sin\alpha\mathbf{u}_1^{\zeta} + \cos\alpha\mathbf{u}_2^{\zeta}) \\ \boldsymbol{\phi}^{\infty} &= \frac{-M}{2I}(x_1\sin\alpha - x_2\cos\alpha)^2\mathbf{n}(\alpha) \end{aligned}\right\} \quad \text{for } \gamma = 0, \tag{16a}$$

where

$$\mathbf{u}_1^{\zeta} = \begin{Bmatrix} \gamma_1 x_1^2 - \gamma_2 x_2^2 \\ (\gamma_6 x_1 + 2\gamma_2 x_2)x_1 \\ (\gamma_5 x_1 + 2\gamma_4 x_2)x_1 \end{Bmatrix}, \quad \mathbf{u}_2^{\zeta} = \begin{Bmatrix} -(2\gamma_1 x_1 + \gamma_6 x_2)x_2 \\ \gamma_1 x_1^2 - \gamma_2 x_2^2 \\ -\gamma_4 x_2^2 \end{Bmatrix}, \tag{16b}$$

and

$$\gamma_i = \hat{S}_{1i}\cos^2\alpha + \hat{S}_{2i}\sin^2\alpha + \hat{S}_{6i}\cos\alpha\sin\alpha, \quad i = 1, 2, 4, 5, 6, \quad \gamma = \gamma_4\sin\alpha + \gamma_5\cos\alpha. \tag{16c}$$

The condition $\gamma = 0$ will always be satisfied for monoclinic materials. By a similar approach, one can obtain the solutions for $\gamma \neq 0$, in which the additional term such as $(ax_1^2 + bx_1x_2 + cx_2^2)\mathbf{i}_3$ should be considered in $\boldsymbol{\phi}'$.

4. FORMULAE FOR SOME SPECIAL HOLES

4.1. *Elliptic holes or cracks* ($\varepsilon = 0$)

When $\varepsilon = 0$, the contour of the hole shown in (1) can be written as

$$x_1 = a\cos\psi, \quad x_2 = ac\sin\psi. \tag{17}$$

The transformation function given in (3) becomes

$$z_\alpha = \frac{a}{2}\left\{(1 - ip_\alpha c)\zeta_\alpha + (1 + ip_\alpha c)\frac{1}{\zeta_\alpha}\right\},$$

or

$$\zeta_\alpha = \frac{z_\alpha + \sqrt{z_\alpha^2 - a^2(1 + p_\alpha^2 c^2)}}{a(1 - ip_\alpha c)}. \tag{18}$$

The square root of a complex number has two distinct values. Hence, ζ_α given above has two distinct values. Neglecting the one located inside the unit circle, we get a single value ζ_α.

4.1.1. *Uniform loading.* The general solutions shown in (2) and the hoop stress shown in (4) can be simplified by using $\varepsilon = 0$ and (5a).

The results are

$$\mathbf{u} = \mathbf{u}^{\infty} - a\,\mathrm{Re}\,\{\mathbf{A}\langle\zeta_z^{-1}\rangle\mathbf{B}^{-1}(\mathbf{t}_2^{\infty} - ic\mathbf{t}_1^{\infty})\},$$

$$\boldsymbol{\phi} = \boldsymbol{\phi}^{\infty} - a\,\mathrm{Re}\,\{\mathbf{B}\langle\zeta_z^{-1}\rangle\mathbf{B}^{-1}(\mathbf{t}_2^{\infty} - ic\mathbf{t}_1^{\infty})\},$$

$$\sigma_{nn} = \cos\theta\{\sigma_1^{(0)} - c\sigma_1^{(3)} + \sigma_2^{(1)}\} + \sin\theta\left\{\sigma_2^{(0)} - \frac{1}{c}\sigma_2^{(3)} - \sigma_1^{(1)}\right\}, \tag{19a}$$

where

$$\sigma_i^{(0)} = \mathbf{n}^{\mathrm{T}}(\theta)\mathbf{t}_i^{\infty}, \quad \sigma_i^{(1)} = \mathbf{n}^{\mathrm{T}}(\theta)[\mathbf{N}_1^{\mathrm{T}}(\theta) - \mathbf{N}_3\mathbf{S}\mathbf{L}^{-1}]\mathbf{t}_i^{\infty}, \quad \sigma_i^{(3)} = \mathbf{n}^{\mathrm{T}}(\theta)\mathbf{N}_3(\theta)\mathbf{L}^{-1}\mathbf{t}_i^{\infty}, \quad i = 1, 2. \tag{19b}$$

For the case of unidirectional tension, the hoop stress can be further simplified as

$$\sigma_{nn}/\sigma^{\infty} = \cos^2(\theta - \alpha) - \{c\cos\theta\cos\alpha + \frac{1}{c}\sin\theta\sin\alpha\}\sigma_0^{(3)} - \sin(\theta - \alpha)\sigma_0^{(1)}, \tag{19c}$$

where

$$\sigma_0^{(1)} = \mathbf{n}^{\mathrm{T}}(\theta)[\mathbf{N}_1^{\mathrm{T}}(\theta) - \mathbf{N}_3(\theta)\mathbf{S}\mathbf{L}^{-1}]\mathbf{n}(\alpha), \quad \sigma_0^{(3)} = \mathbf{n}^{\mathrm{T}}(\theta)\mathbf{N}_3(\theta)\mathbf{L}^{-1}\mathbf{n}(\alpha). \tag{19d}$$

For isotropic materials, we have (Hwu, 1990)

$$\sigma_0^{(1)} = \sin(\theta - \alpha), \quad \sigma_0^{(3)} = -2\cos(\theta - \alpha),$$

and hence,

$$\sigma_{nn}/\sigma^{\infty} = -1 + 2(1 + c)\left[\cos\theta\cos\alpha + \frac{1}{c}\sin\theta\sin\alpha\right]\cos(\theta - \alpha), \tag{19e}$$

which is identical to the one shown in Muskhelishvili (1953).

For circular holes, the solutions can simply be obtained from the formulae given in (17)–(19) with $c = 1$. With this substitution, many equations can be simplified such as $\psi = \theta + \pi/2$, $\rho = a$, etc.

An elliptic hole can be made into a crack of length $2a$ by letting c be equal to zero. From (19) with $c = 0$, one obtains the solutions for crack problems:

$$\mathbf{u} = \mathbf{u}^{\infty} - a\,\mathrm{Re}\,\{\mathbf{A}\langle\zeta_z^{-1}\rangle\mathbf{B}^{-1}\}\mathbf{t}_2^{\infty}, \quad \boldsymbol{\phi} = \boldsymbol{\phi}^{\infty} - a\,\mathrm{Re}\,\{\mathbf{B}\langle\zeta_z^{-1}\rangle\mathbf{B}^{-1}\}\mathbf{t}_2^{\infty}, \tag{20a}$$

where

$$\zeta_z = \frac{1}{a}\{z_z + \sqrt{z_z^2 - a^2}\}. \tag{20b}$$

By using $(20a)_2$ and $\sigma_{i2} = \phi_{i,1}$ with $x_2 = 0$, $|x_1| > a$, the stresses σ_{i2} ahead of the crack tip along x_1-axis can be obtained as

$$\sigma_{i2} = \frac{x_1}{\sqrt{x_1^2 - a^2}}\mathbf{t}_2^{\infty}. \tag{21}$$

The above solution shows that the stresses are singular near the crack tip. With the usual definition, the stress intensity factors are given by

$$\mathbf{K} = \begin{Bmatrix} K_{II} \\ K_I \\ K_{III} \end{Bmatrix} = \lim_{x_1 \to a} \sqrt{2\pi(x_1 - a)}\sigma_{i2} = \sqrt{\pi a}\mathbf{t}_2^{\infty}. \tag{22}$$

Similarly, by using $(20a)_1$ and setting $x_2 = 0^{\pm}$, $|x_1| < a$ where $\pm$ denotes the upper and lower surfaces of the crack, the crack opening displacements $\Delta\mathbf{u}$ are obtained as

$$\Delta\mathbf{u} = \mathbf{u}(x_1, 0^+) - \mathbf{u}(x_1, 0^-) = 2\sqrt{a^2 - x_1^2}\mathbf{L}^{-1}\mathbf{t}_2^{\infty}. \tag{23}$$

In the above, the identity (Ting, 1988)

$$i\mathbf{A}\mathbf{B}^{-1} = \mathbf{L}^{-1}(\mathbf{I} + i\mathbf{S}^{\mathrm{T}})$$

has been used. By applying the virtual crack closure method (Irwin, 1957), the total strain energy release rate G can be calculated as

$$G = \lim_{\Delta a \to 0} \frac{1}{2\Delta a} \int_0^{\Delta a} \Delta\mathbf{u}^{\mathrm{T}}(s - \Delta a)\boldsymbol{\phi}'(s)\, ds = \frac{\pi a}{2}\mathbf{t}_2^{\infty\mathrm{T}}\mathbf{L}^{-1}\mathbf{t}_2^{\infty} = \tfrac{1}{2}\mathbf{K}^{\mathrm{T}}\mathbf{L}^{-1}\mathbf{K}, \tag{24}$$

where s is the distance ahead of the crack tip. For isotropic materials, $\mathbf{L}$ is a diagonal matrix with $L_{11} = L_{22} = \mu/1 - \nu$, $L_{33} = \mu$. Hence,

$$\Delta\mathbf{u} = \frac{2(1-\nu)}{\mu}\sqrt{a^2 - x_1^2}\begin{Bmatrix} \sigma_{21}^{\infty} \\ \sigma_{22}^{\infty} \\ \dfrac{1}{1-\nu}\sigma_{23}^{\infty} \end{Bmatrix}, \quad G = \frac{1-\nu}{2\mu}(K_I^2 + K_{II}^2) + \frac{1}{2\mu}K_{III}^2, \tag{25}$$

which is good for the plane strain condition since Stroh's formalism is derived under the assumption that $\varepsilon_{33} = 0$. To be applicable for the generalized plane stress conditions, a reduced elasticity matrix $\hat{C}_{ij} = C_{ij} - C_{i3}C_{3j}/C_{33}$ should be used.

4.1.2. *Pure bending.* The general solutions shown in (6) and the hoop stress shown in (7) can also be simplified by using $\varepsilon = 0$ and (5a). The results are

$$\mathbf{u} = \mathbf{u}^{\infty} + \frac{Ma^2}{2I}\,\mathrm{Re}\{(c_2 + is_2)\mathbf{A}\langle\zeta_\alpha^{-2}\rangle\mathbf{B}^{-1}\}\mathbf{n}(\alpha),$$

$$\boldsymbol{\phi} = \boldsymbol{\phi}^{\infty} + \frac{Ma^2}{2I}\,\mathrm{Re}\{(c_2 + is_2)\mathbf{B}\langle\zeta_\alpha^{-2}\rangle\mathbf{B}^{-1}\}\mathbf{n}(\alpha),$$

$$\sigma_{nn}\Big/\frac{Ma}{I} = s_0^* \cos^2(\theta - \alpha) + \frac{a}{2\rho}(c^*\sigma_1^{(0)} + s^*\sigma_2^{(0)}), \tag{26a}$$

where

$$s_0^* = \sin(\psi - \alpha) - (1 - c)\cos\alpha\sin\psi,$$

$$s^* = \frac{-1}{2}[1 - c^2 - (1-c)^2\cos 2\alpha]\sin 2\psi + c\sin(2\psi + 2\alpha),$$

$$c^* = \frac{-1}{2}[1 - c^2 - (1-c)^2\cos 2\alpha]\cos 2\psi + c\cos(2\psi - 2\alpha), \tag{26b}$$

and

$$a\sin\psi = \rho\cos\theta, \quad -ac\cos\psi = \rho\sin\theta, \quad \rho = a\sqrt{\sin^2\psi + c^2\cos^2\psi}. \tag{26c}$$

By following a similar procedure to that in Section 4.1.1, the solutions for the cracks subjected to pure bending are obtained as

$$\mathbf{u} = \mathbf{u}^{\infty} + \frac{M(a\sin\alpha)^2}{4I}\,\mathrm{Re}\,\{\mathbf{A}\langle\zeta_\alpha^{-2}\rangle\mathbf{B}^{-1}\}\mathbf{n}(\alpha),$$

$$\boldsymbol{\phi} = \boldsymbol{\phi}^{\infty} + \frac{M(a\sin\alpha)^2}{4I}\,\mathrm{Re}\,\{\mathbf{B}\langle\zeta_\alpha^{-2}\rangle\mathbf{B}^{-1}\}\mathbf{n}(\alpha),$$

$$\mathbf{K} = \frac{-Ma\sqrt{\pi a}\sin^2\alpha}{2I}\mathbf{n}(\alpha), \quad \Delta\mathbf{u} = \frac{-M\sin^2\alpha}{I}x_1\sqrt{a^2-x_1^2}\,\mathbf{L}^{-1}\mathbf{n}(\alpha). \tag{27}$$

It can be seen that Δu_2 will always be negative in either $-a < x_1 < 0$ or $0 < x_1 < a$ if the second component of $\mathbf{L}^{-1}\mathbf{n}(\alpha)$ is not equal to zero, which violates the assumption of fully open crack and the solution is invalid. For this condition, one may assume that the crack is not fully open but with partial contact near the crack tip. If $\{\mathbf{L}^{-1}\mathbf{n}(\alpha)\}_{(2)} = 0$, $\Delta u_2 = 0$ for all x_1 within the crack and hence there is no tendency for the crack to open or close. However, a relative tangential displacement may exist between the crack faces. Therefore, (27) is valid if $\Delta u_2 = 0$ or the negative Δu_2 is increased to a positive value by an applied tensile load.

4.2. *Triangular holes* ($k = 2$)

When $c = 1$ and $k = 2$ the hole has three symmetry axes. With an appropriate selection of the parameter ε, the opening will differ little from an equilateral triangle with rounded corners. The transformation function given in (3) with $k = 2$, in general, is not a conformal mapping function unless $p_\alpha = i$ which is the eigenvalue of isotropic materials. A single-valued ζ_α is then obtained by neglecting the values located inside the unit circle for isotropic materials. For general anisotropic materials, there will be two distinct ζ_α located outside the unit circle. We may choose the one nearest $|\zeta| = 1$ as the mapped point. Hence, the entire z-plane is now mapped onto part of the ζ_α-plane with a one-to-one transformation. The triangular hole is then mapped onto the unit circle and $|\zeta_\alpha| \to \infty$ when $|z| \to \infty$ is also satisfied. However, the ζ_α values may be discontinuous near the critical point ζ_0, which may cause the discontinuity of displacements and stresses. This discontinuity will be discussed in the next section. The definition of the critical point is $(\mathrm{d}z_\alpha(\zeta_\alpha)/\mathrm{d}\zeta_\alpha)|_{\zeta_\alpha=\zeta_0} = 0$.

Similar to the procedure used in the case of elliptic holes, the solutions for triangular holes can be written as follows.

4.2.1. *Uniform loading.*

$$\begin{aligned}
\mathbf{u} &= \mathbf{u}^{\infty} - a\,\mathrm{Re}\,\{\mathbf{A}\langle\zeta_\alpha^{-1}\rangle\mathbf{B}^{-1}(\mathbf{t}_2^{\infty} - ic\mathbf{t}_1^{\infty})\} - a\varepsilon\,\mathrm{Re}\,\{\mathbf{A}\langle\zeta_\alpha^{-2}\rangle\mathbf{B}^{-1}(\mathbf{t}_2^{\infty} + i\mathbf{t}_1^{\infty})\},\\
\boldsymbol{\phi} &= \mathbf{u}^{\infty} - a\,\mathrm{Re}\,\{\mathbf{B}\langle\zeta_\alpha^{-1}\rangle\mathbf{B}^{-1}(\mathbf{t}_2^{\infty} - ic\mathbf{t}_1^{\infty})\} - a\varepsilon\,\mathrm{Re}\,\{\mathbf{B}\langle\zeta_\alpha^{-2}\rangle\mathbf{B}^{-1}(\mathbf{t}_2^{\infty} + i\mathbf{t}_1^{\infty})\},\\
\sigma_{nn} &= \cos\theta[\sigma_1^{(0)} + \sigma_1^{(3)} + \sigma_2^{(1)}] + \sin\theta[\sigma_2^{(0)} + \sigma_2^{(3)} - \sigma_1^{(1)}] + \frac{(1+c)a}{\rho}[-\sin\psi\sigma_1^{(3)} + \cos\psi\sigma_2^{(3)}].
\end{aligned} \tag{28}$$

4.2.2. *Pure bending.*

$$\mathbf{u} = \mathbf{u}^{\infty} + \frac{Ma^2}{2I}\sum_{l=1}^{4}\mathrm{Re}\,\{(c_l + is_l)\mathbf{A}\langle\zeta_\alpha^{-l}\rangle\mathbf{B}^{-1}\}\mathbf{n}(\alpha),$$

$$\boldsymbol{\phi} = \boldsymbol{\phi}^{\infty} + \frac{Ma^2}{2I}\sum_{l=1}^{4}\mathrm{Re}\,\{(c_l + is_l)\mathbf{B}\langle\zeta_\alpha^{-l}\rangle\mathbf{B}^{-1}\}\mathbf{n}(\alpha),$$

$$\sigma_{nn}\Big/\frac{Ma}{I} = s_0^* \cos^2(\theta-\alpha)+\frac{a}{2\rho}(c^*\sigma_0^{(3)}+s^*\sigma_0^{(1)}). \tag{29}$$

4.3. *Oval and square* ($k = 3$)

When $c = 1$ and $k = 3$ there are four symmetry axes and at some values of ε the hole will differ little from a square with rounded corners. If ε is positive the apexes of the square (rounded) are located on axes x_1 and x_2, which consequently run along the diagonals. In the case of negative ε the sides are parallel to the coordinate axes. When $c < 1$ and $k = 3$ we will obtain ovals of a special type.

Similar to triangular holes the transformation function for oval holes is not a conformal mapping in general. The only situation for this to be single-value transformation is isotropic material. For general anisotropic materials, we choose the one located outside the unit circle and nearest $|\zeta| = 1$. The problem of discontinuity will be discussed in the next section. The expressions of $\mathbf{u}$, ϕ and σ_{nn} for oval openings subjected to uniform loading are the same as (28) except that $\langle\zeta_\alpha^{-2}\rangle$ is now changed to $\langle\zeta_\alpha^{-3}\rangle$ and the relation between θ and ψ should be changed according to (5) with $k = 3$. For the case of pure bending, the expressions are exactly the same as (29) except that the index l is now summed for 2, 4 and 6, and the related coefficients c_l, s_l, $l = 2, 4, 6$, s_0^*, c^* and s^* should be changed according to (6c) and (7b). Note that $k-1 = 2$ for $k = 3$. Hence, the terms associated with $k-1$ and 2 should be added together such as $s_2 = \frac{1}{2}[-c+\varepsilon(1+c)]\sin 2\alpha$.

5. VALIDITY AND VERIFICATION

It is well known that the satisfaction of conformal mapping requirement is the key point for the formulae listed in previous sections to be valid. Hence, it is interesting to know when they will be satisfied, and when they are well approximated if they are not satisfied.

5.1. *An anisotropic plate with elliptic holes* (p_α: *complex*, $\varepsilon = 0$)

The transformation function for this condition has been given in (18). The roots of $dz_\alpha(\zeta_\alpha)/d\zeta_\alpha = 0$ are at

$$\zeta_\alpha^2 = \frac{1+ip_\alpha c}{1-ip_\alpha c}.$$

If $p_{\alpha I}$, $p_{\alpha R}$ are, respectively, the real and imaginary parts of p_α, the absolute value of ζ_α^2 is

$$|\zeta_\alpha^2| = \frac{(1-cp_{\alpha I})^2+(cp_{\alpha R})^2}{(1+cp_{\alpha I})^2+(cp_{\alpha R})^2}.$$

Since $p_{\alpha I} > 0$ and $0 < c \leqslant 1$, we have $|\zeta_\alpha^2| < 1$ which leads to $|\zeta_\alpha| < 1$. The roots are therefore located inside the unit circle $|\zeta_\alpha| = 1$ and the transformation function (18) is single-valued and conformal outside the elliptic hole. The solutions provided in Section 4 are therefore exact.

5.2. *An isotropic plate with polygonal holes* ($p_\alpha = i$, ε: *small*)

The transformation function given in (3) can be written as

$$z_\alpha = \frac{a}{2}\left\{(1+c)\zeta_\alpha+(1-c)\frac{1}{\zeta_\alpha}+\frac{2\varepsilon}{\zeta_\alpha^k}\right\}. \tag{30}$$

Differentiating z_α with respect to ζ_α, we have

$$\frac{dz_\alpha}{d\zeta_\alpha} = \frac{a}{2}\left\{(1+c)-(1-c)\frac{1}{\zeta_\alpha^2} - \frac{2\varepsilon k}{\zeta_\alpha^{k+1}}\right\}.$$

If $c = 1$, the roots of $dz_\alpha/d\zeta_\alpha$ are at

$$\zeta_\alpha^{k+1} = \varepsilon k.$$

When the small number ε is chosen such that $\varepsilon < 1/k$, the critical point ζ_0 will be located inside the unit circle $|\zeta_\alpha| = 1$ and the transformation function (30) is single-valued and conformal outside the hole. In the case that $0 \leqslant c < 1$ and ε is comparatively small such that $2\varepsilon k/\zeta_\alpha^{k+1}$ can be neglected, the roots of $dz_\alpha/d\zeta_\alpha$ are at

$$\zeta_\alpha^2 = \frac{1-c}{1+c}$$

which are located inside the unit circle and conformal mapping is obtained. For the other conditions, one can calculate the critical points ζ_0 numerically and check whether $|\zeta_0|$ is smaller than one. From the discussions given above, we know that for isotropic plates the solutions are exact for most cases.

5.3. *An anisotropic plate with polygonal holes* (p_α: *complex*, ε: *small*)

The critical points ζ_0 for the most general conditions considered in (3) are determined by $dz_\alpha/d\zeta_\alpha = 0$, i.e.

$$k\varepsilon(1+ip_\alpha)\zeta_\alpha^{2k} + (1-ip_\alpha c)\zeta_\alpha^{k+1} - (1+ip_\alpha c)\zeta_\alpha^{k-1} - k\varepsilon(1-ip_\alpha) = 0.$$

The product of all critical points is equal to, if $\varepsilon \neq 0$ and $p_\alpha \neq i$,

$$\Pi_{i=1}^{2k}\zeta_i = -\frac{1-ip_\alpha}{1+ip_\alpha},$$

of which the absolute value is greater than one because the imaginary part of p_α is positive. Therefore, one of the critical points will be located outside the unit circle and (3) is not conformal outside the hole for general anisotropic materials.

The occurrence of critical points outside the unit circle means that there will be multiple values of ζ_α, corresponding to one point z_α, located outside the unit circle. If we designate the point nearest the unit circle to be the mapped point, we still have one-to-one transformation. The hole is then mapped onto the unit circle and $|\zeta_\alpha| \to \infty$ when $|z_\alpha| \to \infty$ is also satisfied, which is the requirement for satisfaction of infinity boundary conditions. However, the ζ_α values may be discontinuous near the critical point, which may cause the discontinuity of displacements and stresses. To have a clear understanding of this phenomena, a typical example is shown below.

Example. $k = 2$, $c = 1$, $a = 1$, $\varepsilon = 0.25$, $p_\alpha = 0.6i$ (triangular hole)

The mapping function (3) becomes

$$z_\alpha = \frac{1}{20}\left\{\zeta^2 + 16\zeta + \frac{4}{\zeta} + \frac{4}{\zeta^2}\right\}.$$

The critical points ζ_0 can be calculated numerically by $dz_\alpha/d\zeta = 0$. The results are $\zeta_0 = 0.865$, -7.976, $-0.444 \pm 0.619i$. The plot of this mapping function for real value of ζ is shown in

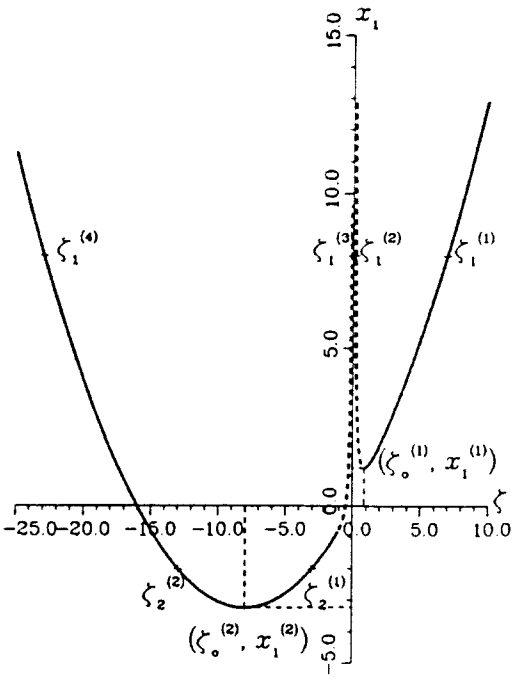

Fig. 1. The plot of the transformation function with real values ($k = 2$, $c = 1$, $a = 1$, $\varepsilon = 0.25$, $p_z = 0.6$).

Fig. 1. If only the points on x_1-axis are considered, Fig. 1 shows that each point on $x_1 > x_1^{(1)}$ ($x_1^{(1)} = 1.228$ is the source point of $\zeta_0^{(1)} = 0.865$) corresponds to four different points ζ ($\zeta_1^{(1)}$, $\zeta_1^{(2)}$, $\zeta_1^{(3)}$, $\zeta_1^{(4)}$) in ζ-domain, which are all real. If we neglect the points located inside the unit circle, i.e. $\zeta_1^{(2)}$ and $\zeta_1^{(3)}$, and designate the point nearest the unit circle to be the mapped point, $\zeta_1^{(1)}$ should be the mapped point chosen for this region. For the range of $x_1^{(2)} < x_1 < x_1^{(1)}$ ($x_1^{(2)} = -3.222$ is the source point of $\zeta_0^{(2)} = -7.976$), each point of x_1 corresponds to two real points ($\zeta_2^{(1)}$, $\zeta_2^{(2)}$) and a pair of complex conjugates which are located inside the unit circle and are not shown in this figure since it is a plot of real values. By neglecting the inside points and choosing the nearest point, the mapped point chosen for this region should be $\zeta_2^{(1)}$. For the point located in $x_1 < x_1^{(2)}$, there are two pairs of complex conjugates. One is inside the unit circle, the other is outside the unit circle. The latter represents two different points ζ_* and $\bar{\zeta}_*$ which have the same distance to the unit circle. If ζ_* is the limiting of the chosen mapped-point corresponding to x_1^+, one may find that $\bar{\zeta}_*$ is the limiting of the chosen mapped-point corresponding to x_1^-. Hence the discontinuity of displacements and stresses may occur in the range of $x_1 < x_1^{(2)}$. In general, if the material eigenvalue p_z is pure imaginary, all coefficients on the right-hand side of eqn (3) are real. Furthermore, if only the points on the x_1-axis are considered, which leads the values of z_z to real numbers, all the coefficients of equation (3) are real. Therefore, if ζ_* is a root of eqn (3), so is $\bar{\zeta}_*$ if ζ_* is not real. The problem of discontinuity may occur if the point nearest the unit circle is not a real number but a pair of complex conjugates.

The discontinuity of displacement at point x_1 for the cases of uniform loading can therefore be written as

$$\Delta\mathbf{u} = \mathbf{u}(\zeta_*) - \mathbf{u}(\bar{\zeta}_*) = 2\sum_{l=1,k} \mathrm{Re}\{(\zeta_*^{\,l} - \bar{\zeta}_*^{\,l})\mathbf{A}\mathbf{q}_l\}.$$

Since $\zeta_*^{\,l} - \bar{\zeta}_*^{\,l}$ is pure imaginary if ζ_* is not real, the only condition for the discontinuity to disappear is that $\mathbf{A}\mathbf{q}_l$ is real. Similarly, for tractions to be continuous at points x_1, $\mathbf{B}\mathbf{q}_l$ should be real. It can easily be proved that the only solution for both $\mathbf{A}\mathbf{q}_l$ and $\mathbf{B}\mathbf{q}_l$ to be real is $\mathbf{q}_l = \mathbf{0}$, which gives $\mathbf{t}_1^r = \mathbf{t}_2^r = \mathbf{0}$. In other words, for general uniform loading conditions, the discontinuity of displacements and tractions occurs at the points of $x_1 < x_1^{(2)}$ along x_1-axis. The solutions provided in previous sections are therefore not exact. However,

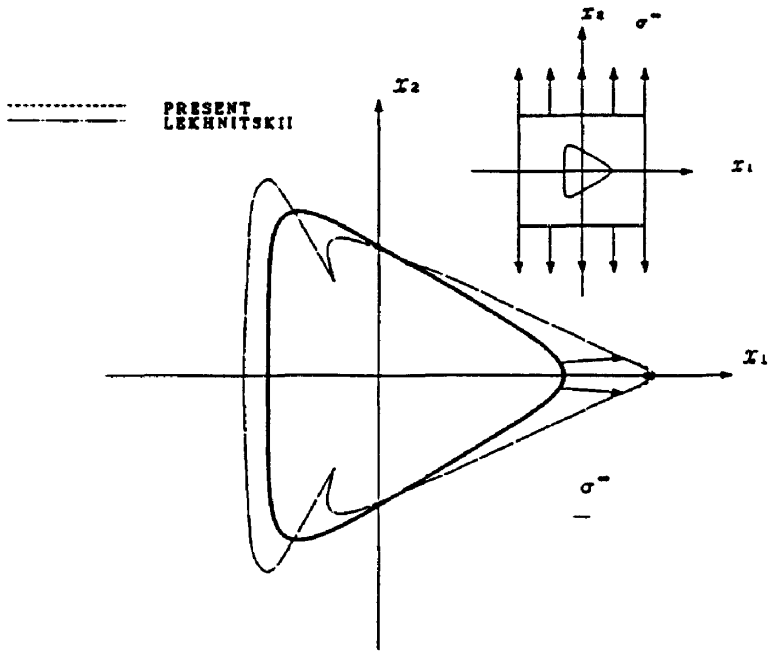

Fig. 2. Hoop stress along the triangular hole under unidirectional tension ($k = 2$, $c = 1$, $a = 1$, $\varepsilon = 0.25$, $\alpha = 90°$, orthotropic materials).

$\zeta_*' - \bar{\zeta}_*' = 0$ when ζ_* is real, i.e. in the range $x_1 > x_1^{(2)}$, and $\bar{\zeta}_*' - \zeta_*' \to 0$, when $\zeta_* \to \infty$, the discontinuity can be neglected for most ranges of x_1 since $x_1^{(2)} = -3.222$ may be treated as a large number relative to unit. The solutions near the hole boundary may therefore be approximated to the exact solutions if the critical points are far away from the unit circle. By comparison with the approximate solutions provided by Lekhnitskii (1968), Figs 2–6 show that these two approximate solutions are almost the same in most cases. Especially, for the triangular holes under unidirectional tension or pure bending shown in Figs 2 and

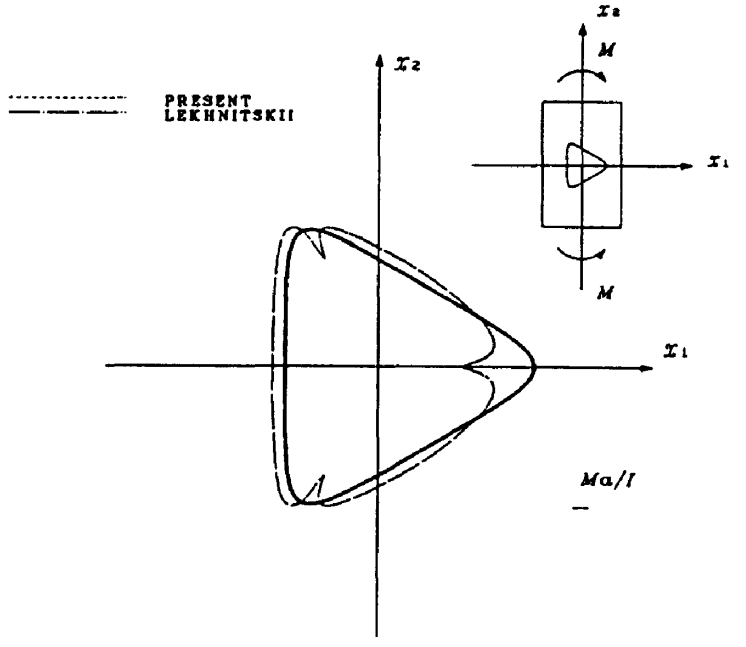

Fig. 3. Hoop stress along the triangular hole under pure bending ($k = 2$, $c = 1$, $a = 1$, $\varepsilon = 0.25$, $\alpha = 90°$, orthotropic materials).

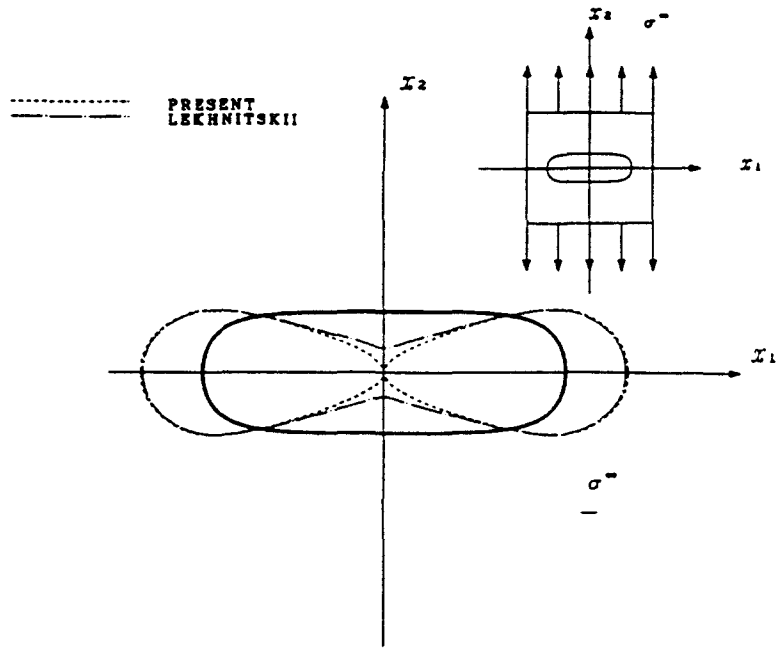

Fig. 4. Hoop stress along the oval hole under unidirectional tension ($k = 3$, $c = 0.36$, $a = 1$, $\varepsilon = -0.04$, $\alpha = 90°$, orthotropic materials).

3, these two solutions are almost exactly the same. The results provided by Lekhnitskii have different expressions for different holes, while the solutions presented in this paper have only one unified expression for various holes. Moreover, in most cases as discussed previously, our results are exact. For example, consider an isotropic plate containing elliptic holes, the hoop stress under unidirectional tension has been given by Muskhelishvili (1953), which is

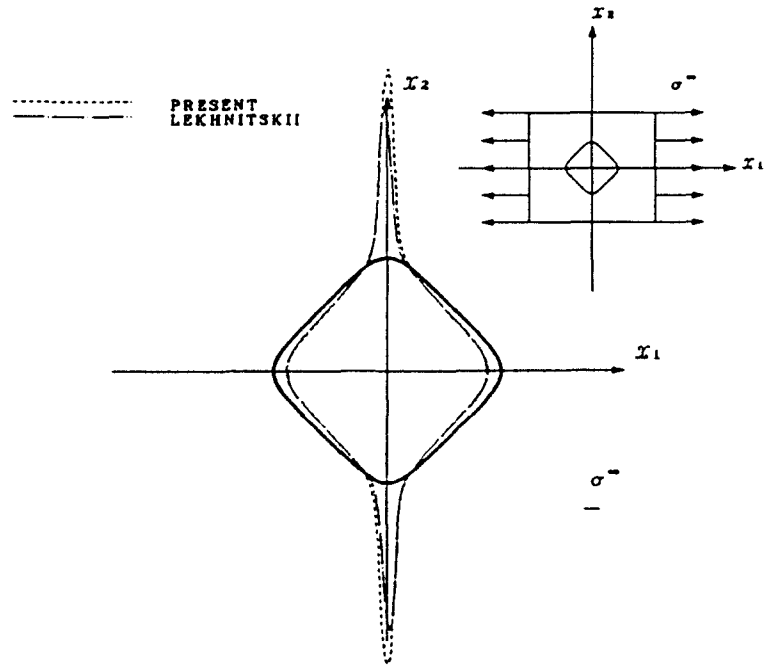

Fig. 5. Hoop stress along the square hole under unidirectional tension ($k = 3$, $c = 1$, $a = 1$, $\varepsilon = 1/9$, $\alpha = 0°$, orthotropic materials).

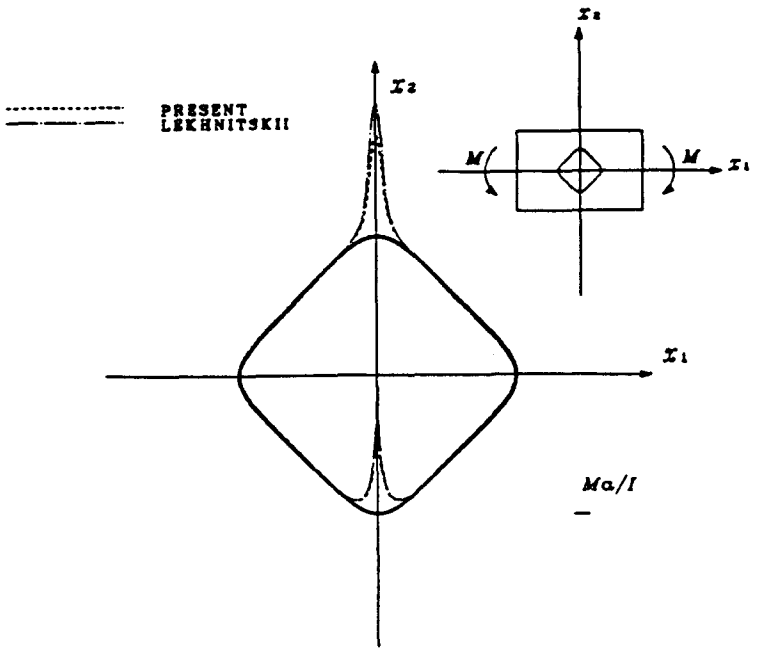

Fig. 6. Hoop stress along the square hole under pure bending ($k = 3$, $c = 1$, $a = 1$, $\varepsilon = 1/9$, $\alpha = 0°$, orthotropic materials).

$$\sigma_{nn} = \sigma^{\infty} \frac{1 - m^2 + 2m\cos 2\alpha - 2\cos 2(\psi - \alpha)}{1 - 2m\cos 2\psi + m^2}, \quad m = \frac{1-c}{1+c}.$$

An equivalent result shown in (19e) can easily be simplified from eqn (4) by substituting the material properties of isotropic media, shape parameter with $\varepsilon = 0$ and the loading conditions given in (12a). The big difference is that the equation provided by Muskhelishvili is valid only for elliptic holes embedded in isotropic media, while eqn (4) is valid for various polygonal holes in general anisotropic media.

The orthotropic materials used in the above figures are taken as

$$E_1 = 22 \times 10^6 \text{ psi}, \quad E_2 = E_3 = 1.54 \times 10^6 \text{ psi}, \quad \nu_{12} = \nu_{13} = \nu_{23} = 0.28,$$
$$G_{12} = G_{13} = G_{23} = 0.81 \times 10^6 \text{ psi},$$

where E, G and ν are, respectively, the Young's modulus, shear modulus and the Poisson's ratio. The subscripts 1, 2 and 3 denote, respectively, the fiber, transverse and thickness directions.

6. CONCLUSIONS

General formulae for polygonal holes in anisotropic media are provided in this paper, from which explicit solutions are derived for some special holes such as ellipses, cracks, triangles, ovals and squares. Moreover, the solutions for the homogeneous media subjected to uniform loading, which includes unidirectional tension (or compression), biaxial loading, inplane shear and antiplane shear, and pure bending are derived in detail for the completeness of the formulae. Due to the nonconformal mapping used in some polygonal holes, the solutions may not be exact in those cases. However, they are well approximated if the critical points of the mapping functions are far away from the holes, which has been verified by comparison with the approximate solution provided by Lekhnitskii (1968).

Acknowledgements—The author would like to thank the National Science Council, Republic of China, for its support through Grant No. NSC 78-0401-E006-31.

REFERENCES

Gao, H. (1991). Stress analysis of smooth polygonal holes via a boundary perturbation method. *J. Appl. Mech.* **58**(3), 851–853.

Hwu, C. (1990). Anisotropic plates with various openings under uniform loading or pure bending. *J. Appl. Mech.* **57**(3), 700–706.

Irwin, G. R. (1957). Analysis of stresses and strains near the end of a crack transversing a plate. *J. Appl. Mech.* **24**, 361–364.

Jones, R. M. (1975). *Mechanics of Composite Materials*. Scripta, Washington, DC.

Lekhnitskii, S. G. (1968). *Anisotropic Plates*. Gordon and Breach, New York.

Muskhelishvili, N. I. (1953). *Some Basic Problems of the Mathematical Theory of Elasticity*. Noordhoof, Groningen.

Savin, G. N. (1961). *Stress Concentration Around Holes*. Pergamon Press, Oxford.

Stroh, A. N. (1958). Dislocations and cracks in anisotropic elasticity. *Phil. Mag.* **7**, 625–646.

Ting, T. C. T. (1988). Some identities and the structures of N, the Stroh formalism of anisotropic elasticity. *Q. Appl. Math.* **46**, 109–120.